International Journal of Nanoelectronics and Materials
Volume 13, No. 3, July 2020 [421-432]

The Effects of Annealing Temperature Dependence on the Doping of Titanium Dioxide (TiO_2) and Reduced Graphene Oxide (rGO) for Perovskite Solar Cell Application

Rafidah Kemat[1,*], Siti Kudnie Sahari[1], and Afiqah Baharin[1]

[1]*Faculty of Engineering, Universiti Malaysia Sarawak (UNIMAS), 94300 Kota Samarahan, Sarawak.*

Received 18 August 2019, Revised 11 February 2020, Accepted 17 May 2020

ABSTRACT

In the present study, reduced Graphene Oxide (rGO) was introduced to Titanium Dioxide (TiO_2) as Electron Transport Layer (ETL) in Perovskite Solar Cell (PSC). TiO_2 doped rGO (TiO_2/rGO) was prepared by doping Titanium (IV) Oxide nanopowder as a precursor for TiO_2 and chemically reduced Graphene Oxide (rGO). The TiO_2/rGO was varied with different annealing temperature and the effects of electrical, structural and optical on TiO_2/rGO of PSC were studied. The surface morphologies of TiO_2/rGO thin films were characterized via X-Ray Diffraction (XRD). Meanwhile, Ultraviolet-visible spectroscopy (UV-Vis) was used to characterize the optical properties of TiO_2/rGO thin films while current-voltage (I-V) analysis was measured by using Keithley Sourcemeter. Structural and morphological evidence from XRD results confirmed that the TiO_2/rGO samples changes from anatase phase to rutile phase as the annealing temperature increased and the average crystalline size of TiO_2/rGO thin films change with the TiO_2 crystalline phase accordingly. The annealing temperature of 550°C exhibits the larger grain size that results in better conductivity, higher light absorption and lower bandgap energy.

Keywords: Annealing Temperature, Doping, Perovskite Solar Cell, Titanium Dioxide, Reduced Graphene Oxide.

1. INTRODUCTION

Solar energy harvesting has been done substantially through photovoltaic devices as energy supply from the sun is reliable, renewable, and sustainable with no worry of depletion [1]. Thin-film based photovoltaics solar cell such as Copper-Indium-Gallium-Selenide (CIGS), Cadmium Telluride (CdTe), Dye-Sensitized Solar Cell (DSSC), Organic Solar Cell and Perovskite Solar Cell (PSC) have caught research attention whereas by 2030 photovoltaic are anticipated as the third of global electricity generation [2].

Perovskite solar cell has shown an increase in power conversion efficiency (PCE) at a phenomenal rate in just seven years as compared to other types of photovoltaics. Perovskite is an organic-inorganic material that has shown capabilities for the use in light-emitting diodes, sensors, field-effect transistors and photodetectors [3]. Despite that, further improvement is important to optimize and enhance the PSC devices operation, stability and device performance. The aim of this research is to construct a photovoltaic device, an organometal halide perovskite solar cell with $CH_3NH_3PbI_3$ as the absorber that coated upon the surface of mesoporous TiO_2/rGO.

*Corresponding author: rafidahkemat@gmail.com

Throughout the years, anatase TiO_2 was found to be the most common material to enhance photocatalytic properties of photoanodes in the solar cell due to its long-term thermodynamic stability, low cost and relatively non-toxicity [4]. However, the drawback is that anatase TiO_2 tend to suffer from high recombination rate of electron-hole pairs with wide bandgap 3.2 eV [5].

On the other hand, graphene has been widely used in applications of optoelectronic and photon energy conversion due to its unique mechanical and electrical properties [6]. Some research studies were conducted and it was reported that rGO nanocomposites were an applicable additive for enhancing the charge collection properties in dye-sensitized solar cells (DSSCs), owing to its ability to effectively reduced the charge-recombination pathways, decrease the leakage current and more recently, TiO_2/rGO composite based blocking layer is negatively effecting the energy barrier and series resistance between TiO_2 [7]. From the literature, it is believed that the combination of TiO_2 and rGO can improve the performance of PSC. Therefore, in this research, rGO was incorporated with TiO_2 and used as photoanodes in PSC. The annealing temperature from 450°C to 650°C dependence on surface morphologies, optical characteristics and current-voltage measurements were studied.

2. EXPERIMENTAL METHODS

2.1 Materials

Chemicals used throughout the experiment are graphite powder, hydrazine solution, dimethylformamide (DMF), titanium Isopropoxide (TTIP), methylammonium lead iodide ($CH_3NH_3PbI_3$), lead (II) iodide (PbI_2), lithium bis(trifluoromethylsulfonyl) imide (Li-TFSI), Spiro-OMeTAD and chlorobenzene purchased from Sigma Aldrich. Potassium permanganate ($KMnO_4$) was supplied from R&M Chemicals while sulfuric acid (H_2SO_4) and hydrochloric acid (HCI) were from Fisher Scientific. Phosphoric acid (H_3PO_4) and hydrogen peroxide (H_2O_2) were bought from Merck. All chemicals were analytical reagents (AR) and have been used without further purification.

2.2 Structure of Perovskite Solar Cell

Figure 1 shows the cross-sectional layer of perovskite solar cell that consists of six different layers. The first layer is the glass substrate layer, then the compact TiO_2 layer. The third layer is the electron transport layer (ETL) which is also called mesoporous layer. Next is the perovskite absorber layer followed by the hole transport layer (HTL) and the last layer is the metal electrode layer.

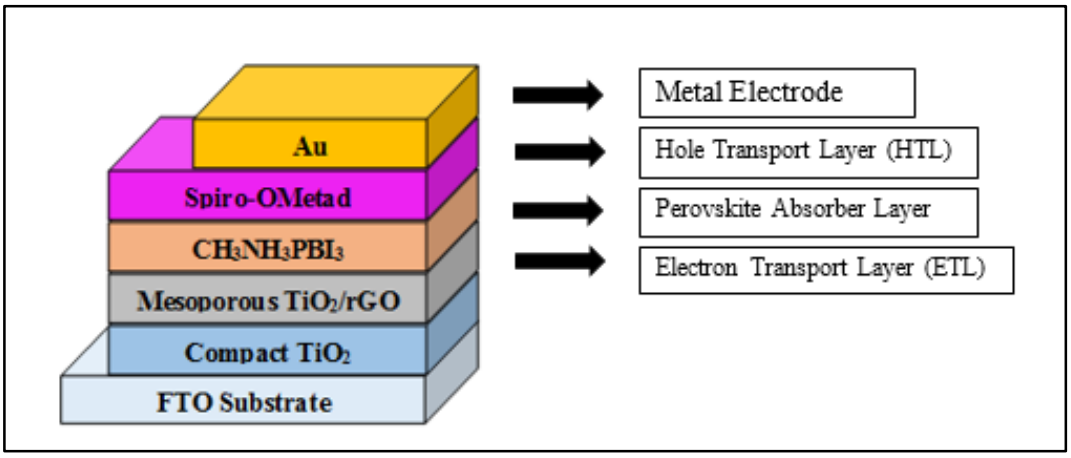

Figure 1. The cross-sectional layer of perovskite solar cell.

2.2.1 Cleaning of Glass Substrate Layer

First, the fluorine-doped tin oxide (FTO) glass was immersed in liquid detergent (DECON 90) and left overnight. Then, the FTO glass was sonicated in acetone, deionized water and 2-propanol each for 10 minutes respectively. The FTO glass was dried using a blower and put inside a UV ozone cleaner for 10 minutes. Lastly, for safety and maintaining the cleanliness of the glass, each of the FTO glass was placed inside a small and tight container.

2.2.2 Deposition of Compact TiO_2 Layer

Titanium Isopropoxide ($Ti(OCH(CH_3)_2)_4$) or also known as TTIP were used as precursor along with absolute ethanol (C_2H_6O), acetic acid (CH_3CO_2H), Triton-X-100 and distilled water. 46.53 mL of ethanol was added to 2.22 mL of TTIP followed by 1.25 mL of acetic acid, 100 µL of distilled water and 50 µL of Triton-X-100 in a beaker. Then, the mixture was stirred at 600 rpm and heated at 60°C for 2 hours before left overnight. Next is the deposition step for the TiO_2 layer. The prepared TiO_2 solution was stirred for 10 minutes in room temperature before being deposited. After that, the solution was spin-coated on top of the conductive side of FTO glass substrate at 3000 rpm for 30 seconds by using vacuum spin coater resulting in a sample size of 2 cm × 2 cm. Then, the sample was annealed on a hot plate at 100°C for 10 minutes and 450°C for 2 hours in the furnace. Lastly, the deposited FTO glass was left to cool down at room temperature.

2.2.3 Electron Transport Layer (ETL)

Titanium Dioxide doped reduced Graphene Oxide (TiO_2/rGO) represents the electron transport layer with annealing temperatures of 450°C, 550°C and 650°C. The preparation of the mesoporous TiO_2/rGO layer is divided into three main parts. The first one was the preparation of graphene oxide solution that chemically reduced to form rGO solution. After that, the preparation of TiO_2 solution before the doping process of TiO_2 and rGO.

2.2.3.1 Preparation of Graphene Oxide (GO)

Graphene Oxide (GO) was synthesized by using Improved Hummer's method. Firstly, 3 g of graphite powder was added to a conical flask which contains 18 g of potassium permanganate ($KMnO_4$). Then, the solution was stirred continuously by using a glass rod for 60 seconds. In another beaker, 360 mL of sulfuric acid (H_2SO_4) was mixed with 40 mL of phosphoric acid (H_3PO_4) and stirred continuously for 60 seconds. After that, the mixture of H_2SO_4 and H_3PO_4 was poured slowly into the conical flask which contained graphite powder and $KMnO_4$ earlier. The colour of the solution changed to dark green at this stage. The solution was then stirred at 80 rpm and heated at 50°C on the hot plate for 12 hours. The mixture was left to cool at room temperature for another 9 hours.

Then, the solution was poured in the beaker that contains ice to stop the oxidation of GO. At the same beaker, 0.75 mL of hydrogen peroxide (H_2O_2) was added. The solution was then stirred for 15 minutes at room temperature. After the colour of the solution changed from dark brown to dark purple, the mixture was centrifuged with deionized (DI) water at 6000 rpm for 30 minutes. 30 minutes was chosen as it's the most ideal time to perfectly removed the impurities in the mixture such as metal ions [22]. The centrifuge process was repeated by using HCl at the same speed and time. The resulting solid was dried at 60°C for 2 hours in an oven and 15 mL of DI water was added to obtain GO solution.

Next, the GO solution was sonicated using normal mechanical sonication becomes clear without particles or residues. The sonication process was carried out at room temperature for 30 minutes. Finally, the GO solution was obtained.

2.2.3.2 Preparation of reduced Graphene Oxide (rGO)

The synthesized GO solution was used to prepare reduced graphene oxide (rGO) solution that chemically reduced by using hydrazine solution. 1 mL of GO solution was added to 50 mL of deionized (DI) water and synthesized via reflux method in an oil bath for equilibrium heat. Then, 17 µL of hydrazine solution was added immediately to the mixture as soon as the stirring and the timer started. The solution was stirred on the hot plate at 300 rpm and heated at 80°C for 12 hours. As a result, rGO was formed in black colour. The solution was then filtered by using filter membrane and dried at room temperature for 24 hours to obtain rGO powder. Lastly, 40 mL of dimethylformamide (DMF) was added to 0.5 g of rGO powder as a solvent to produce an rGO solution.

2.2.3.3 Preparation of Titanium Dioxide (TiO_2) Doped reduced Graphene Oxide (rGO)

Titanium dioxide (TiO_2) was prepared by using titanium (IV) oxide nanopowder as a precursor with the introduction of polyethene glycol in deionized water. To prepare TiO_2 solution, 3 g of titanium (IV) oxide nanopowder was annealed at 450°C, 550°C and 650°C each for 2 hours respectively. For the preparation of 450°C solution, 6 mL of deionized water was added to 2 g of polyethene glycol and stirred for 10 minutes at room temperature. Subsequently, 3 g of titanium (IV) oxide nanopowder that was annealed at 450°C earlier was added to the solution and followed by 5 mL of ethanol, 375 µL of acetic acid and 15 µL of Triton-X-100. After that, the solution was stirred and heated on the hot plate at 300 rpm and 40°C for 30 minutes. The same steps were repeated for both 550°C and 650°C to obtain three different samples.

Then, the doping process was carried out by adding 0.8 mL of prepared rGO solution into 10 mL of the prepared TiO_2 solution. After that, the solution was stirred at 500 rpm and heated at 40°C for 2 hours and left overnight to suppress the bubble in the solution. TiO_2/rGO solution was deposited on top of the compact annealed TiO_2 layer. The solution was spin-coated at 300 rpm for 30 seconds. After that, the deposited FTO substrate was annealed on the hot plate at 100°C for 10 minutes and was left to cool down at room temperature. All of the procedures were carried out in ordinary air condition.

2.2.4 Deposition of Perovskite Layer

Firstly, 0.494 g of methylammonium iodide (CH_3NH_3I) was added to 1.447 g of lead (II) iodide (PbI_2). After that, 1375 µL of γ-butyrolactone analytical standard was added into the solution followed by 1125 µL of dimethylformamide (DMF) with the desired molar ratio at 1:1:1. Next, the solution was stirred at 300 rpm and heated at 60°C for 1 hour. The procedures were conducted in a glove box with very minimal light used in the experimental area as PbI_2 was very sensitive to light and the solution was very sensitive to humidity. The solution of the perovskite phase was then spin-coated on top of the mesoporous TiO_2/rGO layer via spin coating method at 2000 rpm for 45 seconds and annealed from room temperature to 100°C for 15 minutes. Then, the deposited FTO substrate was left at room temperature for the cooling process.

2.2.5 Hole Transport Layer (HTL)

The hole transport layer used was the 2,2',7,7'-tetrakis-(N, N-di-p-methoxyphenylamine)-9,9'-spirobifluorene or also known as spiro-OMeTAD. For the first step, 0.52 g of lithium bis(trifluoromethylsulfonyl) imide (Li-TFSI) was mixed with 1 mL of acetonitrile. In another beaker, 144 µL of 4-tert-butylpyridine was added into 87.5 µL of Li-TFSI that was prepared earlier. Then, 0.3615 g of spiro-OMeTAD in 5 ml of chlorobenzene was mixed in the solution. After that, the solution was stirred at 300 rpm and heated at 40°C for 12 hours. All of the procedure was carried out in a glove box with argon gas. Lastly, the prepared spiro-OMeTAD solution was spin-coated at 4000 rpm for 60 seconds then left dried in a desiccator for overnight.

2.2.6 Preparation of Metal Electrode

The metal electrode used in perovskite fabrication was the gold (Au) metal contacts. The Au was coated by using a gold sputtering machine with aid of homemade mask. The gold sputtering time was 180 seconds to maximize the thickness of Au coated on top of the deposited FTO substrate. Figure 2 shows the schematic illustration for the perovskite solar cell fabrication.

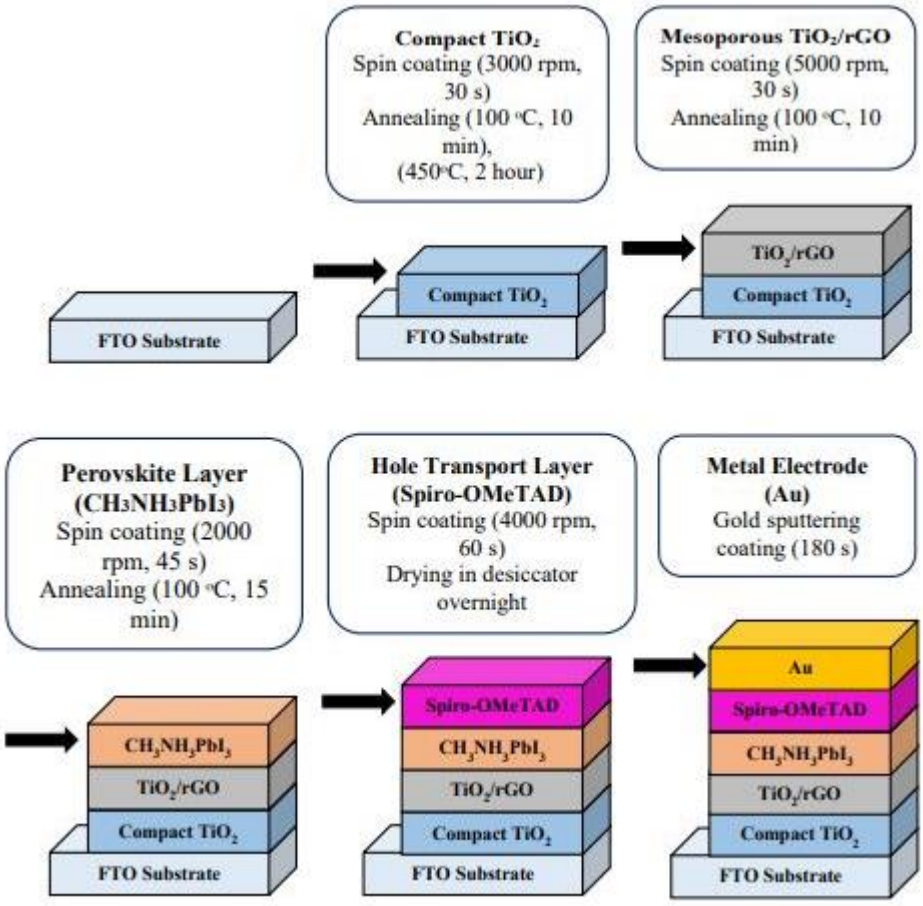

Figure 2. Schematic illustration for perovskite solar cell fabrication.

2.3 Characterization

The surface structure of TiO_2/rGO was observed by using the PANalytical X'PERT PRO MRD PW 3040/60 for X-Ray Diffraction (XRD). The scanning rate employed was 0.033 $^{o}s^{-1}$ in 2Θ range from 20° to 80° with Cu-Kα radiation (λ=1.5406 Å). Then, the optical characterization was evaluated by Ultraviolet-visible spectroscopy (UV-Vis, Shimadzu UV-1800). Lastly, the electrical properties of perovskite solar cell were characterized by using Keithley Sourcemeter (Model 2450) and the measured data were presented as current-voltage (I-V) graph.

3. RESULTS AND DISCUSSION

3.1 Surface Structure

Figure 3 shows the XRD patterns of TiO_2/rGO nanocomposites at different annealing temperatures. The note 'A' indicates TiO_2 in the anatase phase while 'R' means in the rutile phase. The main peak at (A101) diffraction peak at 2θ = 25.3° along with (A004) and (A200). These peaks

matched with the titanium anatase phase represented in International Centre of Diffraction Data (ICDD) standard with file no. 03-065-5714 [8]. TiO_2 in rutile phase also detected by the main (R110) diffraction peak at 2θ = 27.2° along with (R101) which matched the rutile phase in ICDD standard data with file no. 03-065-1118 [9]. Furthermore, it can be observed that the intensity of (A101) peaks becomes weaker as the annealing temperature increase, while the intensity of (R110) and (R101) peaks become sharper and stronger. This shows that the annealing temperature able to transform TiO_2 from anatase to rutile as the temperature increases [17]. Low and the team have reported that the rGO diffraction peaks appeared at 2θ = 24.5° with (002) orientation and at 2θ = 44.5° with (001) orientation [10]. It is believed that rGO stacked together with TiO_2 nanoparticles to form undetectable graphite structure might be due to lower diffraction intensity of rGO and therefore, the presence of rGO diffraction peaks cannot be evidence because it was superposed by the main diffraction peak of TiO_2 at 2θ = 25.3°.

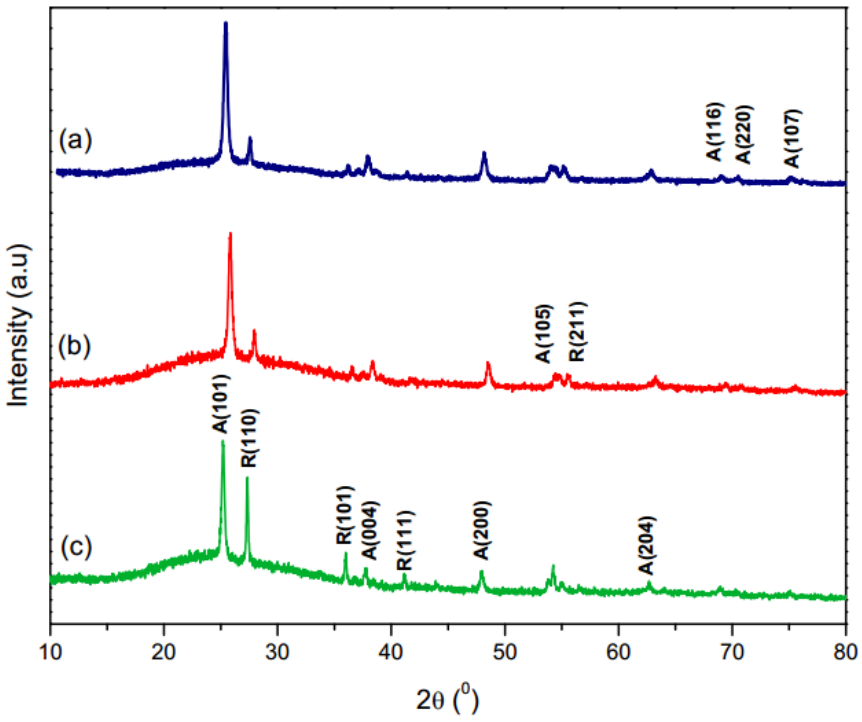

Figure 3. XRD patterns of TiO_2/rGO at different annealing temperatures (a) 450°C, (b) 550°C and (c) 650°C.

The average crystalline particle size is calculated by applying Scherer expressions:

$$D = \frac{0.9\,\lambda}{\beta\cos(\theta)} \tag{1}$$

where λ is the X-ray wavelength (1.5406 Å-Cu K α radiation), β is the line broadening at half maximum intensity (FWHM) and θ is the Bragg angle. Table 1 shows the analysis of XRD patterns.

Table 1 Analysis of XRD patterns

Samples	2θ (°)	d-spacing (Å)	FWHM	Average crystalline size (nm)
450 °C TiO_2/rGO	25.4484	3.4973	0.4324	14.34
550 °C TiO_2/rGO	25.8327	3.4461	0.4645	10.75
650 °C TiO_2/rGO	25.2261	3.5276	0.4119	15.42

The d-spacing obtained were from range 3.44 Å to 3.52 Å which in agreement with previous work that states TiO_2 at (101) peak recorded d-spacing at 3.52 Å [11; 12]. The smallest crystalline size

is 10.75 nm which indicates that 550°C TiO_2/rGO has the highest crystallinity and excellent repeatability compared to other samples [13]. Meanwhile, 650°C TiO_2/rGO has the largest crystalline size which is 15.42 nm due to the increment in temperature-induced grain getting along in phase transition from anatase to rutile phase [14]. It can be concluded that 450°C TiO_2/rGO exist in fully anatase crystallographic form meanwhile 650°C TiO_2/rGO exist in anatase-rutile crystallographic form.

3.2 Optical Characterization

Figure 4 shows the UV-Vis spectra of TiO_2/rGO at different annealing temperatures. There are strong peaks in the range 310-330 nm due to incorporation with rGO that leads to the excitation of electrons from the valence band (O_2p) to the conduction band (Ti_{3d}) during light absorption in the ultra-violet region as discussed in previous research [15,16]. The TiO_2/rGO absorption spectra were illustrated by redshift at 328 nm, 326 nm and 210 nm for TiO_2/rGO annealed at 450°C, 550°C and 650°C which is due to the narrowing of the optical bandgap and lowering the energy thus, extrapolating the linear portion of the curve to zero and positioned it in the visible region. These results were agreed by some researchers [15,17,18]. It can be observed that 550°C TiO_2/rGO has the highest absorbance among all samples while 650°C recorded the lowest absorbance. The lowest absorbance is due to the increasing of particle size which may contribute to the combined effects of particles and crystallinity [19].

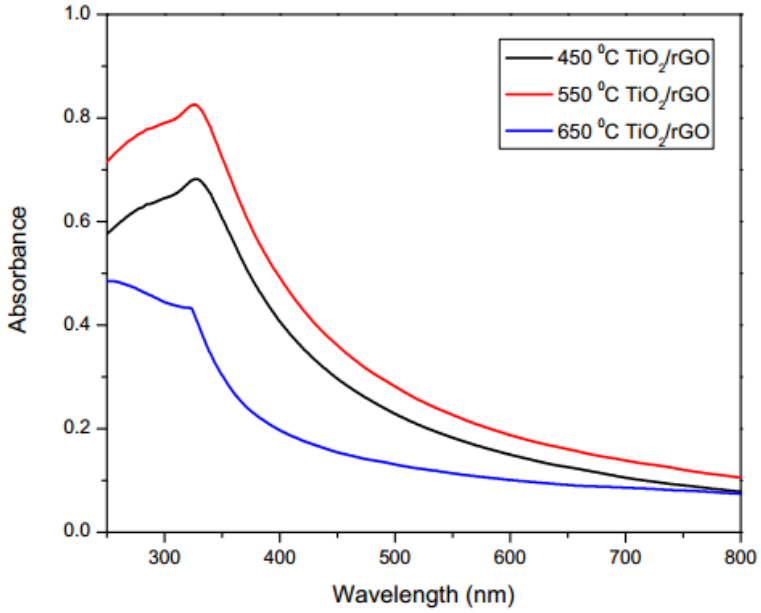

Figure 4. UV-Vis spectra of 450°C TiO_2/rGO, 550°C TiO_2/rGO and 650°C TiO_2/rGO.

In order to obtain the bandgap, the UV-Vis spectra must be converted into Tauc Plot by using the Kubelka-Munk (K-M) formula as the following:

$$\alpha h\nu = A(h\nu - E_g)^2 \quad (2)$$

where α is absorbance coefficient, h is the plank's constant (4.136 x 10^{-15} eV), A is the constant (~1), v is the speed of light (3×10^8 ms^{-1}), E_g is the bandgap energy and n is the indirect allowed transition. Table 2 shows the values of the bandgap for all samples. The lowest bandgap is 2.48 eV which belongs to 550°C TiO_2/rGO while 650°C TiO_2/rGO resulted in the highest bandgap of 2.97 eV. The bandgap obtained for 450°C TiO_2/rGO and 550°C TiO_2/rGO are lower than the

reported bandgap value for anatase TiO_2 of 3.2 eV that implies, the formation of Ti-C and Ti-O-C bonds during doping process of TiO_2 and rGO [20].

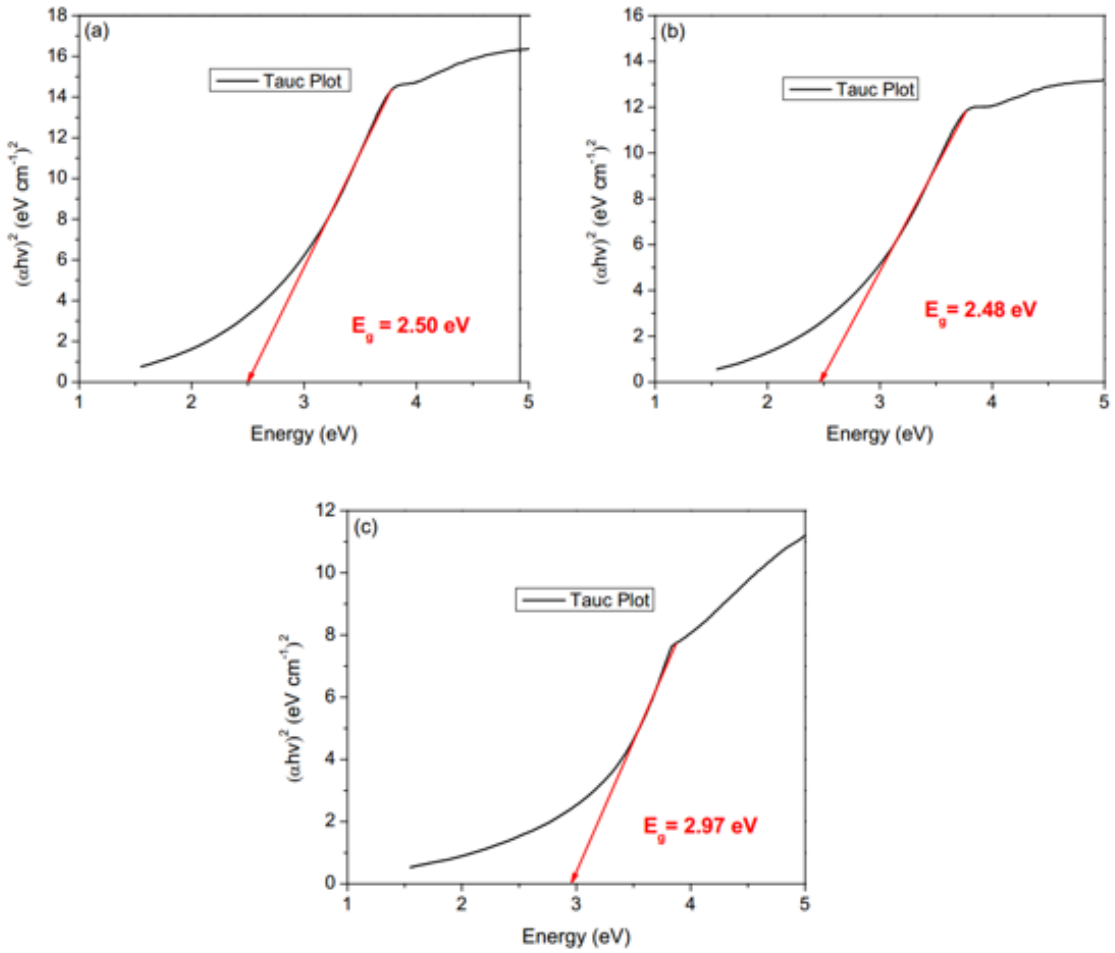

Figure 5. Tauc Plot of TiO_2/rGO at different annealing temperatures.

Table 2 Energy band gap of TiO_2/rGO at different annealing temperatures

Samples	Bandgap (eV)
450 °C TiO_2/rGO	2.50
550 °C TiO_2/rGO	2.48
650 °C TiO_2/rGO	2.97

3.3 Electrical Properties

The I-V plot of perovskite solar cell at different annealing temperature is illustrated in Figure 6. The calculated electrical properties are tabulated in Table 3. It can be observed that 550°C TiO_2/rGO shows the highest current at 9.41 mA. From the I-V plot, 550°C TiO_2/rGO also has the highest conductivity at 18.83 × 10^{-3} S/cm. The result obtained is higher than the reported conductivity value for pure TiO_2 and rGO [21,22]. This results may be due to the effect of incorporation of rGO and TiO_2.

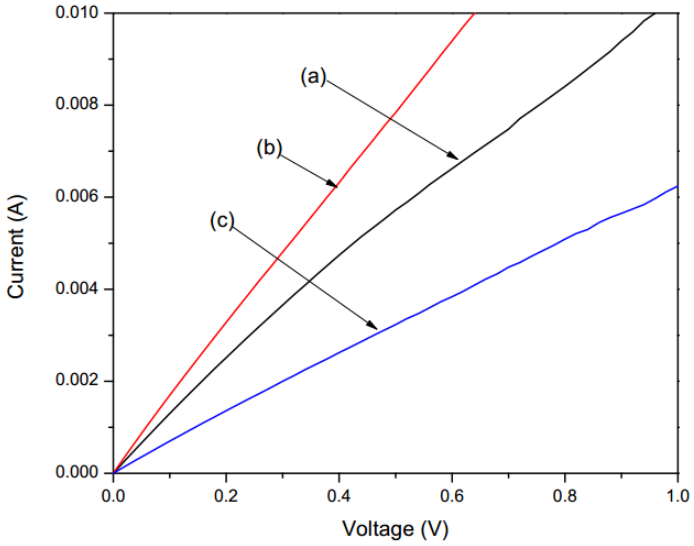

Figure 6. I-V characteristic of TiO_2/rGO PSC at different annealing temperature (a) 450°C TiO_2/rGO, (b) 550°C TiO_2/rGO and (c) 650°C TiO_2/rGO.

Other than that, as TiO_2/rGO PSC fabricated with spiro-OMeTAD as hole transport layer, the increment in conductivity also attributed to the suppressed charge recombination between TiO_2/rGO and spiro-OMeTAD [23]. The thick mesoporous TiO_2/rGO layer helps to lower the possibility of hole transferred to FTO electrode which favouring the electron transportation [24]. This leads to reducing the recombination of hole and transport carriers at the PSC interfaces. To sum up, the electrical performances obtained are in agreement with theoretical studies whereas the doping of rGO in TiO_2 with different annealing temperature and its fabrication in PSC will increase its photocatalytic performance in photovoltaics.

Table 3 Electrical properties of TiO_2/rGO PSC at different annealing temperatures

Samples	Current (mA)	Resistance (Ω)	Conductance (10^{-2} S)	Resistivity (Ω.cm)	Conductivity (10^{-3} S/cm)
450°C TiO_2/rGO	6.45	93.023	1.075	77.489	12.91
550°C TiO_2/rGO	9.41	63.761	1.568	53.114	18.83
650°C TiO_2/rGO	3.84	156.25	64	130.156	7.683

4. CONCLUSION

The study on the effects of TiO_2 doped rGO with annealing temperature dependence and its fabrication in perovskite solar cell has demonstrated remarkable findings. The effect of annealing temperature on structural, optical and electrical properties was studied. The phase transition from anatase to rutile at the annealing temperature of 550°C resulted in the lowest bandgap energy of 2.48 eV. The incorporation of rGO and TiO2 for photoanode has higher conductivity than pure rGO and pure TiO2 that believed can increase the performance of PSC.

ACKNOWLEDGEMENTS

The authors would like to acknowledge Universiti Malaysia Sarawak and the Ministry of Education Malaysia for funding this work under Fundamentals Research Grant Scheme (FRGS) F02/FRGS/1617/2017.

REFERENCES

[1] I. K. Popoola, M. A. Gondal & T. F. Qahtan, "Recent progress in flexible perovskite solar cells: Materials, mechanical tolerance and stability," Renewable and Sustainable Energy Reviews **82** (2018) 3127-3151.

[2] M. A. Green, A. Ho-Baillie & H. J. Snaith, "The emergence of perovskite solar cells," Nature Photonics **8**, 7 (2014) 506-514.

[3] T. T. Ava, A. A. Mamun, S. Marsillac & G. Namkoong, "A review: Thermal stability of Methylammonium Lead Halide Based Perovskite Solar Cells," Applied Sciences **9**, 1 (2019) 188-199.

[4] X. Kang, S. Liu, Z. Dai, Y. He, X. Song & Z. Tan, "Titanium Dioxide: From Engineering to Applications," Catalysts **9**, 2 (2019) 191-200.

[5] L. Tan, W. Ong, S. Chai & A. Mohamed, "Reduced graphene oxide-TiO_2 nanocomposite as a promising visible-light-active photocatalyst for the conversion of carbon dioxide," Nanoscale Research Letters **8**, 1 (2013) 465-460.

[6] K. T. Cho, G. Grancini, Y. Lee, D. Konios, S. Paek, E. Kymakis & M. K. Nazeeruddin, "Beneficial role of reduced graphene oxide for electron extraction in highly efficient perovskite solar cells," ChemSusChem **9**, 21 (2016) 3040-3044.

[7] X. Wang, H. Sarvari, H. Dang & Z. Chen, "Optik Evolution characteristics of perovskite solar cells in air and vacuum environments," Optik-International Journal for Light and Electron Optics **150**, (2017) 111-116.

[8] H. Awang & N. I. Talalah, "Synthesis of reduced graphene oxide-titanium (rGO-TiO_2) composite using solvothermal and hydrothermal methods and characterized via XRD and UV-Vis," Natural Resources **10**, 2 (2019) 17-28.

[9] C. Fan, C. Chen, J. Wang, X. Fu, Z. Ren, G. Qian & Z. Wang, "Black hydroxylated titanium dioxide prepared via ultrasonication with enhanced photocatalytic activity," Scientific Reports **5**, 1 (2015) 13-22.

[10] F. W. Low, "Study of reduced graphene oxide film incorporated of TiO_2 species for efficient visible light driven dye-sensitized solar cell," Journal of Materials Science: Material in Electronics **28**, 4 (2017) 3819-3836.

[11] F. F. Targhi, Y. S. Jalili & F. Kanjouri, "$MAPbI_3$ and $FAPbI_3$ perovskite as solar cells: Case study on structural, electrical and optical properties," Results in Physics **10**, (2018) 616-627.

[12] S. V. Kite, D. J. Sathe, S. S. Patil, P. N. Bhosale & K. M. Garadkar, "Nanostructured TiO_2 thin films by chemical bath deposition method for high photoelectrochemical performance," Materials Research Express **6**, 2 (2018) 264-271.

[13] F. W. Low, C. W. Lai & S. B. Hamid, "One step hydrothermal synthesis of titanium dioxide decorated on reduced graphene oxide for dye-sensitized solar cells application," International Journal of Nanotechnology **15**, 3 (2018) 78-86.

[14] A. S. Bakri, M. Za. Sahdan, F. Asriyanto, N. A. Raship, N. D. Said, S. A. Abdullah & M. S. Rahim, "Effect of annealing temperature of titanium dioxide thin films on structural and electrical properties," AIP Conference Proceedings **17**, 8 (2017) 324-330.

[15] F. W. Low & C. W. Lai, "Reduced graphene oxide decorated TiO_2 for improving dye-sensitized solar cells (DSSCs)," Current Nanoscience **14**, (2018) 1-6.

[16] D. Kim, S. J. Yang, Y. S. Kim, H. Jung & C. R. Park, "Simple and cost-effective reduction of graphite oxide by Sulphuric acid," Carbon **50**, 9 (2012) 3229-3232.

[17] E. Nouri, M. Reza & P. Lianos, "Impact of preparation method of TiO_2-rGO nanocomposite photoanodes on the performance of dye-sensitized solar cells," Electrochimica Acta **219**, (2016) 38-48.

[18] K. Park, Q. Zhang, B. B. Garcia & G. Cao, "Effect of annealing temperature on TiO_2-ZnO core-shell aggregate photoelectrodes of dye-sensitized solar cells," Journal of Physical Chemistry C **115**, 11 (2011) 4927-4934.

[19] Y. Liu, L. Tian. X. Tan, X. Li & X. Chen, "Synthesis, properties and applications of black titanium dioxide nanomaterials," Science Bulletin **62**, 6 (2017) 431-441.

[20] E. Nouri, M. Reza & P. Lianos, "Improving the stability of inverted perovskite solar cells under ambient conditions with graphene based inorganic charge transporting layers," Carbon **126**, (2018) 208-214.
[21] A. Harry, M. Sawawi, M. Kashif, S. K. Sahari & M. Rusop, "Optical, Electrical and Structural Investigation on Different Molarities of Titanium Dioxide (TiO_2) via Sol-Gel Method," Journal of Telecommunication, Electronic and Computer Engineering **8**, 12 (2016) 87-91.
[22] E. Jaafar, M. Kashif, S. K. Sahari & Z. Ngaini, "Study on morphological, optical and electrical properties of graphene oxide (GO) and reduced graphene oxide (rGO)," Materials of Science Forum **917**, (2018) 112-116.
[23] G. Niu, W. Li, F. Meng, L. Wang, H. Dong & Y. Qiu, "Study on the stability of $CH_3NH_3PbI_3$ films and the effect of post modification by aluminium oxide in all-solid-state hybrid solar cell," Journal of Materials Chemistry A **2**, 3 (2014) 705-710.
[24] K. Li, J. Xiao, X. Yu, T. Li, D. Xiao, J. He & Y. Cheng, "An efficient, flexible perovskite solar module exceeding 8% prepared with an ultrafast PbI_2 deposition rate," Scientific Reports **8**, 1 (2018) 1-8.